SHEAR-OUT FAILURE BEHAVIOUR OF SURFACE STRUCTURED METALLIC Z-REINFORCEMENTS FOR CFRP LAMINATES AND JOINTS

M. Juergens[1], M. T. von Hafe Pérez Ferreira da Silva[1] and E. Ladstaetter[2]

[1]Airbus Group Innovations, 81663 Munich
Email: michael.m.juergens@airbus.com, Web Page: http://www.airbusgroup.com
[2]Institute for Carbon Composites, Technical University of Munich, Boltzmannstraße 15, 85748 Garching, Germany
Email: ladstaetter@lcc.mw.tum.de, Web Page: http://www.lcc.mw.tum.de

Keywords: metallic z-reinforcements, bridging law, delamination resistance, CFRP

Abstract
Shear-out behavior of interleaving metallic z-reinforcements for carbon fiber reinforced polymer (CFRP) laminates and joints is determined and respective energy absorbing mechanisms are described with respect to the metallic materials and means of surface pretreatment applied. Milli-, micro- and nanoscaled oxide morphologies induced on titanium and stainless steel surfaces result from mechanical, wet-chemical and physical surface pretreatments. A low delta in thermal expansion with regard to the surrounding CFRP and a high macro roughness of the reinforcement surface are clearly proven to feature the highest level of energy absorption during pull-out tests. Surface analyses support the assumption of laser-induced nanostructure's scale and morphology to provide good adhesion properties but not to allow macroscopic friction between metal surface and epoxy resin.

1 Introduction

Various z-reinforcement technologies have been developed in order to improve the delamination properties of adhesively bonded fibre-reinforced polymer laminates. Considerable progress is documented for methods such as z-pinning [1],[2], HYPER joints [3] and cold metal transfer (CMT) welded pins [4]. A cost- and time-efficient joining technique features a low-thickness sheet of stainless steel or titanium with out-of-plane bent reinforcing elements. These spikes are positioned between two carbon fiber reinforced polymer (CFRP) adherents before or during the co-bonding process [5],[6], creating a secondary load bridging path and thus working as damage arresting features to the joint through a meso-scale mechanical interlocking. Related research revealed traction loads to significantly increase through-thickness properties for z-pinned laminates by resisting crack opening (Mode I) and crack sliding (Mode II) [1],[7],[8]. Contrary to single carbon fiber pins, the continuous metallic structure of the sheet bending technique allows to benefit from the increased surface by pretreating it and thus to enable further mechanical interlocking with the surrounding epoxy resin / adhesive on a milli-, micro- or even nanoscale level [9].
This work is dedicated to investigating on the impact of scaled metallic reinforcement surfaces' morphologies and composition on the spikes' failure behavior exposed to shear-out loading conditions. Related research was dedicated to Mode II multi-pin testing of carbon fiber z-pins [10], primarily stating a bilinear bridging law to describe the occurring traction forces. In a first stage, the z-pin is fully bonded to the surrounding resin and bridging force is determined by elastic deformation of the z-pin. Once interfacial shear stresses exceed interfacial shear strength, debonding of the z-pin from the laminate is initiated and one half of the spike is being pulled out of the laminate asymmetrically during the second stage. Yet, plastic deformation of metallic z-pins and poor adhesion properties cause an early entry into a non-linear behaviour at the end of stage one, contrary to carbon fiber z-pins. Final

Excerpt from ISBN 978-3-00-053387-7

pull-out in stage two is dominated by friction and plastic deformation, leading to a linear / non-linear functional relationship for carbon fiber / metallic z-pins respectively.
Material and structural properties of the metallic z-reinforcements discussed in this work [5],[6],[9] deviate significantly from the conventional z-pinning technology. Thus, a dedicated multi-pin test method was developed respecting the specifics of the integrated reinforcement structure. On a macroscopic level the impact of the reinforcements' coefficient of thermal expansion (CTE) and Young's modulus on the bridging law is investigated on. Moreover, means of mechanical, wet-chemical and physical surface pretreatment are applied to describe interfacial phenomena between reinforcements and the surrounding resin on a milli-, micro- and nanoscale [9]. A number of techniques were proven to provide enhanced long-term durable adhesion on titanium and stainless steel [11]-[13]. Major drawbacks of wet-chemical processes like environmental issues and unique bath setups for varying alloys incentivized the development of alternative physical techniques [12],[14]. Laser induced nanostructuring of a titanium α+β-alloy surface was developed to improve joint strength due to an increased surface area [14],[15]. Substrate material contamination removal and chemical activation by the energy introduced were studied in [9],[16]. Related investigations on surface modified metallic reinforcements proved interfacial mechanical interlocking on a milli- and nanoscale to significiantly increease delamination resistance compared to conventional pretreatments [9].
This paper provides an extension to those findings, generating an understanding of the mechanical and chemical interfacial interactions, i.e. adhesion and frictional properties between polymer and metallic reinforcement surface on a single (multi) pin level. Shear-out tests identify dominating failure modes driving the Mode II delamination behavior of laminates featuring multiscale structured reinforcements. Results reveal the necessity to distinguish between mechanisms of adhesion and mechanical interlocking to be the dominating energy dissipating mechanism.

2 Manufacturing

The applied approach of integrating the reinforcing metal sheets into a prepreg laminate is highlighted in [5],[9]. Continuous sheets were subsequently stamped and bent in an integrated tooling developed by Hölzel Stanz- und Feinwerktechnik GmbH & Co. KG (Wildberg (DE)). For each configuration a set of five specimens was manufactured in the same curing cycle as depicted in Figure 1.

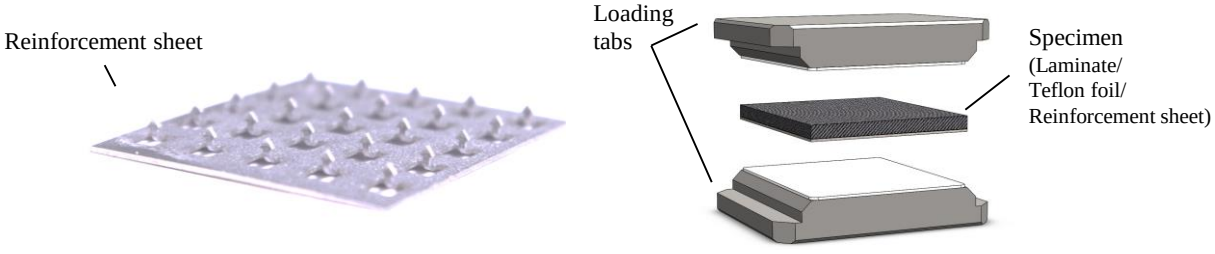

Figure 1: a) reinforcement sheet and b) specimen composition

Pretreated reinforcement sheets penetrate the laminate during the curing cycle, simply realigning (not cutting) the fibers. A thin release film covering the carrying sheet ensures the spike surface only to mechanically and chemically interact with the surrounding resin. Stainless steel loading tabs adhesively bonded on top and bottom side of the specimens allow simple mounting and an even stress distribution during testing.

3 Experimentation

3.1 Materials and geometry

Specimens were manufactured from HexPly® M21/198/T800S medium grade unidirectional prepreg, provided by Hexcel Composites GmbH, Stade (DE). A {0/90/0/-45/+45}S layup was used to compose laminates with a nominal thickness of 1.93 mm.

Excerpt from ISBN 978-3-00-053387-7

Commonly used α+β-alloys lack of cold formability, hence a meta-stable β-alloy Ti 15-3 (AMS 4914A, aerospace specification) by Timet Inc., Exton, PA (US) was chosen to manufacture reinforcement sheets of 0.4 mm thickness each. SAE 304 stainless steel provides a more cost-efficient benchmark, featuring a higher CTE, Young's modulus and density though. Due to the specimens' comparatively small dimensions, CTE induced deformations could not be confirmed at all [9].

3.2 Mechanical surface pretreatment: grit blasting

Mechanically treated sheets were grit-blasted (GB) with Al_2O_3 (grain size: 250-500 µm, blasting pressure: 7 bar) to roughen and increase the active surface. Plasma irradiation was applied in a consecutive step to chemically convert process-related contaminations into species that are harmless to the joining process.

3.3 Wet-chemical surface pretreatment: alkaline etching

All sheet surfaces were cleaned prior to etching with an alkaline solution of P3 Almeco 18, 30 g/l (Henkel AG & Co. KGaA, Düsseldorf (DE)) at 60 °C ± 3 for 15 min.
Etched stainless steel and titanium sheets were exposed to a 40/52 % HF/HNO_3 solution and Turco 5578® 500 g/l (Henkel) respectively. The acid etching process was set up at RT for 5 min, whereas the alkaline process was performed under 95 °C for 5 min.

3.4 Physical surface pretreatment: laser irradiation

Short pulsed laser irradiation (wavelength: 1064 nm) was generated by a Powerline E25 system ($Nd:YVO_4$, Rofin-Sinar Laser GmbH, Hamburg (DE)). A set of parameters for laser induced nanostructuring was developed by Kurtovic [14] for Ti-6Al-4V which was applied for the physical pretreatment of both, beta-alloy Ti 15-3 and SAE 304 stainless steel. The spike carrying sheet was focused in a 90° angle to the normal incidence in ambient atmosphere. Geometrical constraints impede a contingence angle of > 60° which was proven to be sufficient to enable the energy input required for structure thicknesses of > 150 nm [9]. Typical morphologies for laser pretreated surfaces are contrasted to structures resulting from mechanical and wet-chemical treatments in Figure 2 [9].

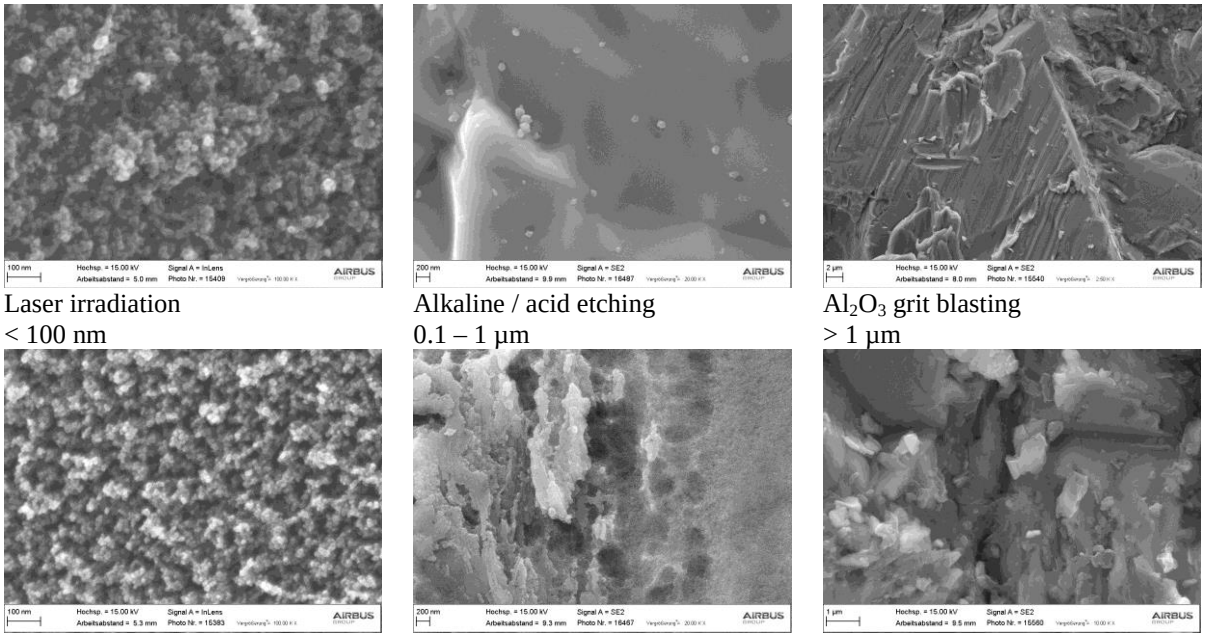

Figure 2: Size and shape in a high magnification detail of Ti 15-3 (top) and SAE 304 (bottom) surface structure morphologies investigated [9]

Excerpt from ISBN 978-3-00-053387-7

Both, mechanical interlocking of epoxy resin and / or adhesive with the nano-cavities created and chemisorption due to an increased hydroxyl group concentration were determined to be dominating mechanisms of adhesion [9],[14].
Alkaline or acid etched surfaces reveal a microscaled morphology, similar to investigations in [14],[17]. Surfaces are rather smooth and flat for SAE 304; pickling environment impedes oxide layer formation due to its chromium dissolving characteristic [18]. On a titanium α+β-alloy substrate, oxide thicknesses of 20-30 nm were documented [17], showing a more rugged morphology.
Titanium reinforcements show fragmented surfaces post grit blasting and a brittle fracture-like morphology due to its lower ductility compared to the austenitic SAE 304. Al_2O_3 residues are indicated on both materials by randomly distributed bright spots [9].
An additional set of configurations featuring release agent (RA) treated spikes (both geometries and materials) was manufactured to separate the effect of adhesion from the mechanism of macroscopic mechanical interlocking of the spikes.

3.5 Multi pin pull-out testing, Mode II

A 10 kN machine (Z010, Zwick GmbH & Co. KG, Ulm (DE)) was set up at a constant crosshead displacement rate of 1 mm/min to test all specimens until failure or total spike pull-out; force was introduced at the outer flanks of the loading tabs (see Figure 1 b and Figure 3)).

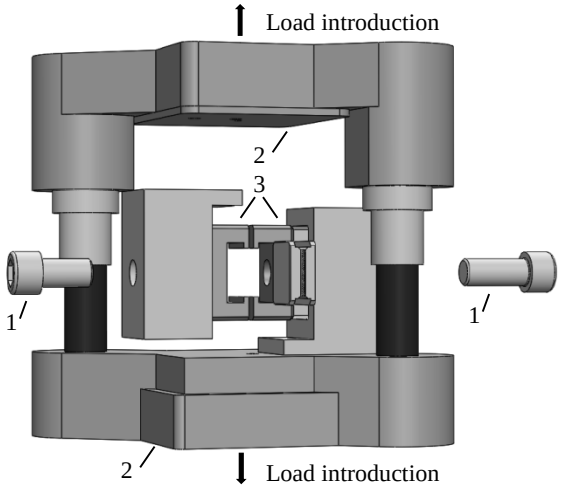

Figure 3: Multipin shear-out test setup (1 – fixing screws, 2 – ball bearing supported upper and lower structure of test fixture, 3 – specimen mount)

Spike array selection in related research on CF multi pin pull-out tests ranges from a 3 x 3 up to a 7 x 7 layout [19],[20]. For this work, a 5 x 5 spike on 25 mm x 25 mm configuration was chosen in order to stick close to the areal density of 1.2 % investigated in [6],[9]. Average bridging load per single reinforcement is derived by dividing overall force applied on the specimen by the number of spikes. Since raw test data supplied by the load cell includes the deformation of the experimental setup, additional tests were conducted on bonded only tabs (without specimen) and the displacements recorded were subtracted from the original plots.

4 Results

4.1 Reinforcement failure behavior

Light microscopic analysis post failure revealed spike deformation behaviour as depicted schematically in Figure 4.

Excerpt from ISBN 978-3-00-053387-7

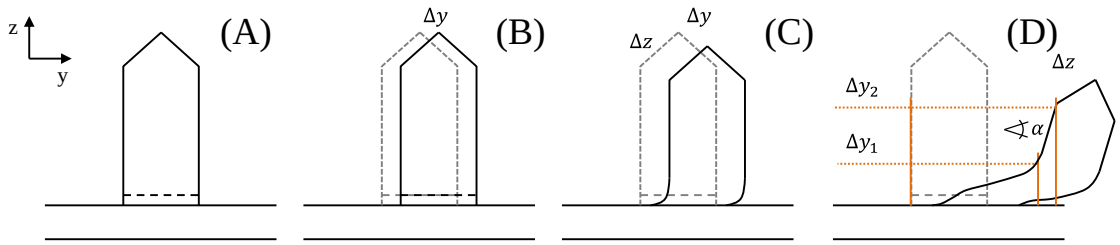

Figure 4: Spike deformation behaviour during shear-out off the laminate

Elastic deformation from the initial state (A) to state (B) was observed during testing as a lateral offset between laminate and reinforcement sheet. Post relaxation of the experimental setup the initial state (A) was visually restored. State (C) results from plastic deformation in the area around spike's bending radius. Further loading leads to a more pronounced deflection of the top (Δy_2) of the spike with regard to the middle (Δy_1) and bottom part which experiences a significant constriction.
Sandblasting of the spike surface results in the largest residual deformations of Δy_1 = 1335 µm ± 51 and Δy_2 = 1923 µm ± 59 (Ti-15-3) or Δy_1 = 1540 µm ± 121 and Δy_2 = 2089 µm ± 81 (SAE 304). Considering the ration $\Delta y_2/\Delta y_1$, higher values of max. 21 % and 9 % in average were documented for titanium spikes, leading to an increased slope α of the upper part of the spike, beyond Δy_1. Among the configurations featuring titanium reinforcments, a significant share of spikes of up to 78 % (grit blasting) were sheared-off during testing, compared to only 2 % for the stainless steel spikes.

4.2 Force vs. displacement behavior and energy absorption

Curves constituting the functional relationship $F(\delta)$ are depicted in Figure 5, each representing a combination of reinforcement material and surface pretreatment applied.

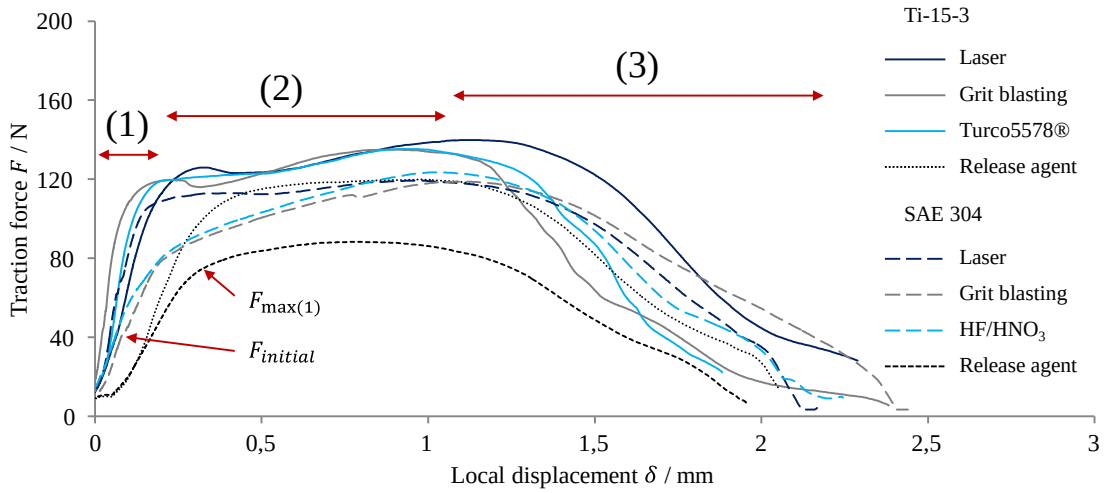

Figure 5: Impact of surface pretreatment on the functional relationship $F(\delta)$ for metallic z-reinforcments during shear-out off a CFRP laminate

A generic shape of the curves can be clearly identified and a classification of the failure behaviour into three substages is proposed, contrary to the bilinear law described in [10].

1 Linear increase of the traction force $F(\delta)$ applied featuring a saddle point, particularly pronounced for the titanium reinforcements
2 Linear increase of the traction force $F(\delta)$
3 Final, non-linear increase of the traction force $F(\delta)$ to the maximum and consecutive, continuous load drop

Excerpt from ISBN 978-3-00-053387-7

Discontinuities ($F_{initial}$) in stage (1) of the recorded curves are documented for the grit blasted surfaces only, but were acoustically perceptible for all configurations, except for the release agent treated and acid etched spikes. Configurations featuring release agent treated reinforcements show their max. force values in stage (2) already, whereas surface structured spikes lead to a further increase until final failure in stage (3). The formation of a saddle point between stages (1) and (2) is subject to significant scatter. However, in a generic assessment, this phenomenon is more pronounced for the (surface structured) titanium reinforcements compared to their stainless steel counterparts. In this context, max. traction force in stage (1) $F_{max(1)}$ obviously exceeds values of those configurations that do not show a saddle point, as indicated in Figure 5.
Nanostructured reinforcements (laser irradiation) lead to superior stiffness values in stage (1) of 943,29 N/mm ± 152,79 and 517,69 N/mm ± 159,04 compared to mechanically (916,98 N/mm ± 333,43 und 429,79 N/mm ± 146,62) and wet-chemically (849,40 N/mm ± 183,43 und 437,39 N/mm ± 105,21) treated spikes for titanium and stainless steel alloys respectively. A drop is noticeable of stiffness before and after the initially described discontinuity for the grit blasted stainless steel spikes from 863,30 N/mm ± 257,12 to values reduced by approx. 50 %.
Stainless steel reinforcements furthermore show inferior load bearing capacity, decreasing with the morphology size. On the other hand, laser pretreatment leads to superior traction forces $F_{max(1)}$ and F_{max} for titanium reinforcements. Basically, the ratio of max. traction forces F_{max} vs. energy absorbed during shear-out is slightly higher for Ti-15-3 spikes, particularly for grit blasted surfaces. Lowest values ($F_{max(1)}$, F_{max}, energy absorbed) were recorded for release agent treated spikes independent of the alloy applied. Yet, respective gaps to surface structured reinforcements were much larger for stainless steel; release agent treated titanium spikes lead to values close to wet-chemically and mechanically treated counterparts.

5 Discussion

Spike deformation (see Figure 4) is assigned to the three major stages of the functional relationship F(δ) in Figure 6.

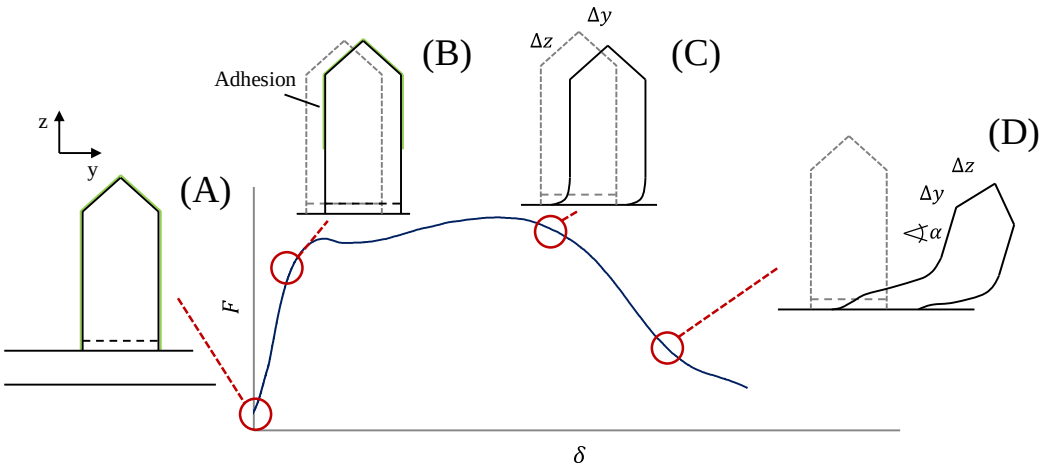

Figure 6: Failure behaviour of z-reinforcements during shear-out off the laminate: (A) adhesively integrated spike; (B) partially/entirely debonded and elastically deformed spike; (C) entirely debonded, elastically and plastically deformed spike (particularly in the area of the bending radius); (D) constriction in the area of the bending radius prior to final pull-out or shear-off.

All configurations experience plastic deformation (stages (2) and (3), see Figure 5) due to testing kinematics. Elastic pull-out ist prevented by constrained degrees of freedom in z-direction. The acoustically perceptible discontinuity in stage (1) was identified as initial adhesion failure, growing upwards the spike surface during spike's elastic (stage (1)) and plastic (stage (2)) deformation until condition (C).

Excerpt from ISBN 978-3-00-053387-7

In earlier investigations [10], a phenomenon was designated "ploughing", describing a load drop post resin fragmentation around the spike root which is one possible explanation for the saddle point in the transistion from stage (1) to stage (2). Moreover, good adhesion properties and low thermally induced residual stresses between spike and resin allow an even stress distribution among all 25 spikes / specimen and a high load level at $F_{max(1)}$, explaining this phenomenon for titanium spikes in general and for laser pretreated Ti-15-3 reinforcements in particular. Both, a low gap of laminate's and spike's CTE and good adhesion properties furthermore significantly increase stiffness of the trilinear relationship in stage (1). As results in [21] indicate, it is most of all the increased slope in stage (1) that dominates Mode II delamination properties of a CFRP/CFRP joint, reinforced with the technology discussed in this work. Superior adhesion properties on metallic surfaces were proven to result from a nanoscaled oxide morphology on the one hand, allowing mechanical interlocking with the surrounding resin (mechanical adhesion). In addition, a cleaned and activated surface promotes chemical adhesion by covalent links between polymeric resin and metal oxide [9][14][15][17]. Mechanical and wet-chemical treatments provide morphologies on a larger scale. However, surface chemistry reveals a lower degree of activation and decontamination and hence reduces spike surface's potential to chemically interact with the polymer. Furthermore, a higher surface roughness might provide better frictional properties during pull-out, but the mechanism of mechanical adhesion was proven to benefit most from a structure featuring small cavities [9][14][17].

6 Conclusions and outlook

A trilinear bridging law was established to describe force displacement behaviour during shear-out testing of metallic z-reinforcements for CFRP laminates. Due to metal's plasticization a significant deviation was noticed with regard to the bilinear functional relationship for conventional carbon z-pinning. Material choice strongly determines failure behaviour. A low reinforcement's CTE induces less residual stresses and increases system stiffness during an initial stage of elastic deformation as part of the trilinear shear-out process. Improved adhesion properties by nanostructuring the spike surface further increase stiffness and Mode II delamination properties of which a strong correlation is suggested.
Future work will be dedicated to assessing the impact of moisture ingress on Mode I pull-out and delamination properties of such reinforced laminates and joints. A qualitative model will be provided to establish a link between the bridging law on a multipin level and delamination properties under Mode I and Mode II loading conditions.

Acknowledgments

We want to express our appreciation to the Federal Ministry of Education and Research, Germany, (BMBF) for funding this research within the TransHybrid project.

References

[1] A.P. Mouritz. Review of z-pinned composite laminates. *Composites*, 38A:2383-2397, 2007.
[2] I.K. Partridge, D.D.R. Cartié, T. Bonnington. *Manufacture and performance of z-pinned composites*. In: G. Shonaike, S. Advani, eds. Advanced polymeric composites. CRC Press, 2003.
[3] P.N. Parkes, R. Butler, D.P. Almond. Growth of damage in additively manufactured metal-composite joints. *Proceedings of the 15th European Conference on Composite Materials ECCM15, Venice, Italy,* June 2012.
[4] S. Stelzer, S. Ucsnik, J. Tauchner, T. Unger, G. Pinter. Novel composite-composite joining technology with through thickness reinforcement for enhanced damage tolerance. *Proceedings of the 19th International Conference on Composite Materials ICCM-19, Montreal, Canada,* July 2013.
[5] A.C. Nogueira, K. Drechsler, E. Hombergsmeier. Analysis of the Static and Fatigue Strength of a Damage Tolerant 3D-reinforced Joining Technology on Composite Single Lap Joints.

Excerpt from ISBN 978-3-00-053387-7

Proceedings of the 53rd AIAA/ASME/ASCE/AHS/ASC Structures, Structural Dynamics and Materials Conference, Honolulu, HI, United States, April 2012.

[6] M. Juergens, A.C. Nogueira, H. Lang, E. Hombergsmeier, K. Drechsler. Influence of an optimized 3d-reinforcement layout on the structural mechanics of co-bonded CFRP joints. *Proceedings of the 16th European Conference on Composite Materials ECCM16, Seville, Spain,* June 2014.

[7] D.D.R. Cartié. *Effect of Z-Fibres ™ on the Delamination Behaviour of Carbon Fibre / Epoxy Laminates.* Doctoral thesis. Cranfield University Library, 2000.

[8] A.P. Mouritz. Delamination properties of z-pinned composites in hot-wet environment. *Composites*, 52A:134-142, 2013.

[9] M. Juergens, A. Kurtovic, T. Mertens, A.C. Nogueira, H. Lang, M. Kolb, P. Strobach, E. Hombergsmeier, K. Drechsler. Effect of surface treatment for metallic z-reinforcements on interlaminar fracture toughness of CFRP/CFRP joints. *Proceedings of the 30th SAMPE30 Conference, Baltimore, MD, United States,* May 2015.

[10] D.D.R. Cartié, B.N. Cox, B.N. Fleck. Mechanisms of crack bridging by composite and metallic rods. *Composites*, 35A:1325-1336, 2004.

[11] A. Baldan. Review: adhesively bonded joints and repairs in metallic alloy, polymers and composite materials: adhesives, adhesion theories and surface pretreatment. *Journal of Materials Science*, 39:1-49, 2004.

[12] R. Broad, J. French, J. Sauer. CLP new, effective, ecological surface pretreatment for highly durable adhesively bonded metal joints. *International Journal of Adhesion and Adhesives,*19:193-198, 1999.

[13] F. Bouquet, J.M. Cuntz, C. Coddet. Influence of surface treatment on the durability of stainless steel sheets bonded with epoxy. *Journal of Adhesion Science and Technology*, 6:233-242, 1992.

[14] A. Kurtovic, E. Brandl, T. Mertens, H.J. Maier. Laser induced surface nano-structuring of Ti-6Al-4V for adhesive bonding. *International Journal of Adhesion and Adhesives,* 45:112-117, 2013.

[15] P. Molitor, T. Young. Investigations into the use of excimer laser irradiation as a titanium alloy surface treatment in a metal to composite adhesive bond. *International Journal of Adhesion and Adhesives*, 24:127-134, 2007.

[16] R. Rechner, I. Jansen, E. Beyer. Influence on the strength and aging resistance of aluminium joints by laser pre-treatment and surface modification. International Journal of Adhesion and Adhesives, 30: 595-601, 2010.

[17] T. Mertens, F.J. Gammel, M. Kolb, O. Rohr, L. Kotte, S. Tschöcke, S. Kaskel, U. Krupp. Investigation of surface pre-treatments for the structural bonding of titanium. *International Journal of Adhesion and Adhesives,* 34:46-54, 2012.

[18] B.S. Covino, J.V. Scalera, T.J. Driscoll, J.P. Carter. Dissolution behavior of 304 stainless steel in HNO_3/HF mixtures. *Metallurgical Transactions,* 17A:137-149, 1986.

[19] S.-C. Dai, W. Yan, H.-Y. Liu, Y.-W. Mai. Experimental study on z-pin bridging law by pullout test. *Composites Science and Technology,* 64:2451-2457, 2004.

[20] A.P. Mouritz. Delamination properties of z-pinned composites in hot-wet environment. *Composites*, 52A:134-142, 2013.

[21] M. Juergens, A. Kurtovic, T. Mertens, M. Kolb, D. Greitemeier, H. Lang, E. Hombergsmeier, K. Drechsler. Influcence of surface treatment and design of 3D-reinforcements on delamination resistance & mechanical properties of CFRP/CFRP joints under static & fatigue loading. *Proceedings of the 20th International Conference on Composite Materials ICCM-20, Copenhagen, Denmark,* July 19-24 2014.

Excerpt from ISBN 978-3-00-053387-7